Ultrasonic characterization of 3-D thermal turbulence confined by moderate aspect ratio box

Megumi Akashi[1], Yuji Tasaka[1], Yuichi Murai[1], Takatoshi Yanagisawa[2]

[1] Laboratory for Flow Control, Hokkaido University, Sapporo 060-8628, Japan
[2] Department of Deep Earth Structure and Dynamics Research , Japan Agency for Marine-Earth Science and Technology (JAMSTEC), Yokosuka 237-0061, Japan

Ultrasonic velocity profiling was performed in a square Rayleigh-Bénard (RB) cell confined by a moderate aspect ratio box using water as working fluid. Rayleigh number, Ra, was in a range from 8.8×10^5 to 1.3×10^7 and the regime of thermal turbulence were expected. Spectra of velocity were calculated to capture transition of spatiotemporal characteristics. Velocity maps show that cellular flow vanishes, and instead large scale flow arises from coalescence of transient plumes and drifts in a direction at $Ra = 2.4\times10^6$. As reached $Ra = 1.3\times10^7$, this large scale flow is divided to several pieces and their arrangement change temporally. Spectra also represent modification of shapes by the transition. The energy spectrum obtained at $Ra = 8.8\times10^5$ has a clear gap of energy between large and small scales of flow unlike that the others have simple decrease of the energy from large to small scales. The power spectrum obtained at $Ra = 1.3\times10^7$ shows a clear peak at much lower frequency in addition to oscillations corresponding to behaviors of local structures. This represents the temporal characteristic of 3-D motions in large scale flow and it may be considered to be unique to RB convection confined by a moderate aspect ratio box.

Keywords: Natural convection, Thermal turbulence, Large scale flow, Flow reversal

1. Introduction

Rayleigh-Bénard convection in fluid layers heated from below is the most fundamental thermal convection and has been a preferred subject for the study of turbulence. In this system, cellular convection with horizontal length scale comparable to the layer depth occurs for small enough values of the Raleigh number. As the Rayleigh number is increased, cellular flow vanishes and is replaced by a random array of transient plumes and the regime achieves thermal turbulence. In further increase, these plumes coalesce and drift in a direction near the bottom and in the opposite direction near the top of the layer. In the case of water having Prandtl number $Pr = 7.0$, this large scale flow is formed around Rayleigh number $Ra = 2.4\times10^6$ in the experiment [1]. At high Rayleigh number conditions, plumes separating from the thermal boundary layer interact with the mean shear flow. The interactions tilt the plumes, generate a Reynolds shear stress and maintain the large scale flow against viscous dissipation. Even with considerations of such high Rayleigh number effects, there is a room for discussions, for example, why such transition occurs and how the direction of the large scale flow is determined. The investigation of the behavior of large scale flow mostly has been limited to convection confined by boxes of aspect ratio close to unity. And spontaneous flow reversals of the large scale flow were detected and analyzed in the particular case of the two-dimensional (2-D) rectangular geometry [2]. The occurrence of flow reversals sensitively depends on the aspect ratio, because the lateral wall of box is decisive for the large scale flow. Therefore, much interest centers to investigate the behavior of large scale flow in 3-D thermal turbulence confined by a moderate aspect ratio box from both points of view in engineering and geophysics.

Point measurements have been employed to investigate the behavior of thermal turbulence, e.g. thermocouples and a laser doppler anemometer, and have detected statistic features of thermal turbulence [3,4]. In the present report, ultrasonic velocity profiling (UVP) is used to visualize the behavior of large scale flow in thermal turbulence confined by a moderate aspect ratio box as time-space velocity maps. Besides, we obtain spatiotemporal characteristics of thermal turbulence quantitatively by calculating spatial spectra and power spectra from the time-space velocity maps using discrete Fourier transform. Less effort has been made to investigate transition of spatiotemporal characteristics of 3-D thermal turbulence as increasing Rayleigh number experimentally. And it is important to understand how large scale flow occurs and how the structure of large scale flow changes as increasing Rayleigh number. In this study, a range of Rayleigh numbers from 8.8×10^5 to 1.3×10^7 is investigated.

Rayleigh-Bénard convection in this system is described by two non-dimensional numbers; Rayleigh number ($Ra = g\beta D\Delta TL^3/\kappa\nu$) indicating the balance between buoyancy and viscous force and Prandtl number ($Pr = \kappa/\nu$), where g and ΔT are gravitational acceleration and vertical temperature difference of the fluid layer, β, κ, and ν are bulk modulus, thermal diffusivity and kinematic viscosity of the test fluid, respectively.

2. Experimental apparatus and method

2.1 Apparatus

Figure 1 shows illustrations of the experimental setup. The fluid layer has a horizontal cross section of 200×200 mm^2 and the height is $L = 40$ mm, giving an

aspect ratio five. The working fluid is water with a mean temperature of 22 ℃, having Pr = 6.8. The upper and bottom plates of the fluid layer are made of copper with the temperature of each plate are maintained by circulating water. The experimental conditions regarding temperature are listed on Table 1. Here T_c and T_h mean the temperatures at the top and bottom plate, respectively, and the vertical temperature difference of the fluid layer is $\Delta T = T_h - T_c$. The Rayleigh number is controlled by ΔT in a range from $Ra = 8.8\times10^5$ to 1.3×10^7, where thermal turbulence regime is expected and large scale flow occurs as reached $Ra = 2.4\times10^6$. The side walls of the fluid layer are 10 mm thick Teflon block providing good thermal insulation. In addition, the outside temperature is kept at a mean temperature of the test fluid by air conditioning in the room.

Table 1: Experimental conditions regarding temperatures

	T_h(℃)	T_c(℃)	ΔT(℃)	Ra
Exp.(a)	22.5	21.5	1	8.8×10^5
(b)	23.5	20.5	3	2.6×10^6
(c)	26	18	8	7.0×10^6
(d)	30.5	15.5	15	1.3×10^7

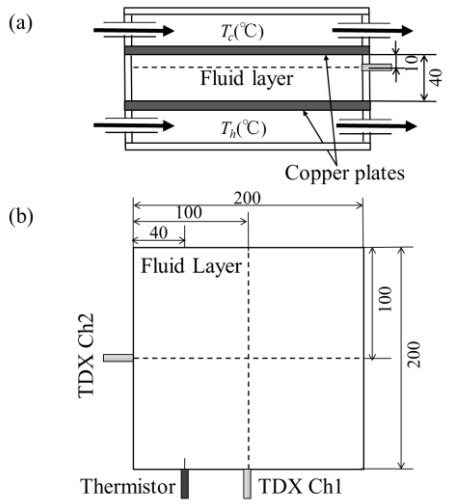

Figure 1: (a) Side view of the setting of the experiment. The dimensions are in mm. (b) Top view of the fluid layer. Dash lines show an ultrasonic beamline of the transducer.

2.2 Measurement method

UVP was used to measure the velocity field of the flow in thermal turbulence. The equipment for velocity measurement was a UVP-Duo (Met-Flow S.A); the basic frequency and effective diameter of the ultrasonic transducer are 4 MHz and 5 mm. Two transducers (TDX Ch1, TDX Ch2) were set in holes on the sidewalls and had direct contact with the fluid to improve transmission of ultrasonic wave as shown in Fig. 1. Each transducer was located with its center 10 mm away from the upper plate. With this condition, UVP has the velocity resolution of 2.7 $\times10^{-1}$ mm/s, the spatial resolution of 9.7 $\times10^{-1}$ mm and the temporal resolution of 2.1 s. The flow velocities were measured along two beamlines from those transducers which cross perpendicularly at the center of the fluid layer. Therefore, it was possible to deduce 3-D structure of thermal turbulence with their time variations. Also spatial–temporal characteristic of the thermal turbulence were captured quantitatively by calculating spatial spectrums and power spectrums of the velocity fluctuations from time-space velocity map through DFT. As ultrasonic reflection particles, HP20SS, were suspended in the fluid. The particles have 63-153 μm in diameter and about 1.01 in specific gravity. To measure temperature oscillations simultaneously, a thermistor probe was installed in the fluid layer close the sidewall as shown Fig.1 with setting height 10 mm below the top plate. Besides, two thermistor probes were also installed to monitor the temperatures of top and bottom plates. The sampling rate and temperature resolution on the measurements are 2.0 Hz and 0.01℃, respectively

3. Results

3.1 Multiple-scale flow patterns in thermal turbulence

Figure 2 shows time-space velocity maps of the flow for 1000 s observed by the UVP at four Rayleigh numbers, (a) $Ra = 8.8\times10^5$, (b) 2.6×10^6, (c) 7.0×10^6 and (d) 1.3×10^7. The horizontal axis is the time and the vertical axis is the distance from the respective transducers. The UVP measures horizontal velocity along the ultrasonic beamlines, and the direction and magnitude of the horizontal flow velocity are displayed in gray scale: White (minus) indicates flow toward the transducer and black (plus) indicates flow away from the transducer. Time-space velocity maps obtained by the transducers are in the velocity range and show similar patterns at each Rayleigh number. This suggests that the flow structure is almost isotropic (no dependence on sides of the box). We, therefore, display the velocity maps obtained from one transducer in Fig. 2.

In the case of (a) $Ra = 8.8\times10^5$, there are relatively clear boundaries of positive and negative velocity component area on the velocity map and each velocity band is in size of 50 – 100 mm. This suggests that a 3-D cellular structure remains with indistinct boundaries. The cells are organized by transient plumes and the boundaries are fluctuating. Positions of the cells are kept for about several hundred seconds.

In the case of (b) $Ra = 2.6\times10^6$ and (c) $Ra = 7.0\times10^6$, positive and negative velocity parts move on the map mainly toward the transducer through measurement lines. The parts have around 50 mm in size and may correspond to local convection structure organized by transient plumes. The direction is kept the same throughout measurement time and this carrier flow indicates large scale flow in thermal turbulence. In comparison with condition (b), the velocity map for condition (c) has smaller structures, but takes common

characteristics of motions of the local structures.

As reached (d) $Ra = 1.3\times10^7$, unlike other cases, motion of the local structure is not uniform. The large scale flow seems to be divided in to two or three pieces and corresponding flow direction changes temporally. A comparison of the velocity maps through the conditions from (a) to (d) indicates that the magnitudes of flow velocities become larger at higher Rayleigh number, while the sizes of local structures become smaller and the fluctuations of flow velocity have shorter periods. To characterize variations of these scales, in the next section, spatial spectrum and power spectrum calculated from time-space velocity maps and temperature fluctuations are investigated.

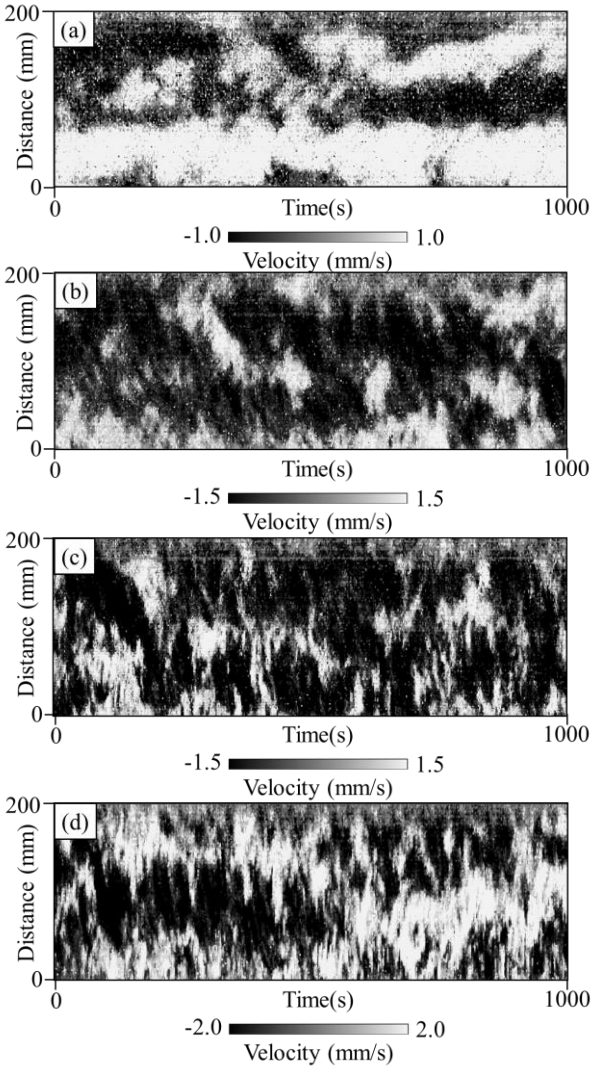

Figure 2: Time-space velocity map of the horizontal flow velocities measured by Ch1 for 1000 s at (a) $Ra = 8.8\times10^5$, (b) 2.6×10^6,(c) 7.0×10^6 and (d) 1.3×10^7

3.2 Time-space characteristics of thermal turbulence

Spectral analysis is the most straightforward tool to understand complex structures of thermal turbulence. Figure 3(A) shows time-averaged energy spectral density, average of energy spectra obtained at each time step, at each Rayleigh number. The spectra show continuous variation indicating feature of thermal turbulence. These are classified into two shapes, the spectrum obtained at (a) $Ra = 8.8\times10^5$, and the ones for larger *Ra* conditions. The former has a peak at the wave number of 0.01 mm^{-1} whose wavelength is 100 mm and indicates the sizes of 3-D cells observed in the time-space velocity map in Fig. 2(a). Also it has inflection point around 0.07 mm^{-1} while the other spectra show almost simple decreases. The latter has the maximum energy at the longest wave number of 0.005 mm^{-1} whose wavelength is 200 mm. This corresponds to size of the large scale flow and these agree with observations in the velocity map shown in Fig. 2.

To elucidate instantaneous features of scale of flows, Fig. 3(B) shows comparison of instantaneous energy spectral densities at (a) $Ra = 8.8\times10^5$ and (c) $Ra = 7.0\times10^6$. The spectra at (a) show peaks at the wavelength of about 100 mm corresponding to the 3-D cells. Besides, they have several spectral peaks at higher wave numbers and these indicate the sizes of transient plumes. The spectra at (c) $Ra = 7.0\times10^6$ have an additional peaks at the wavelength of about 50-100 mm that correspond to local structures. These sizes of local structures have deviation and change every moment. Thus the corresponding peaks disappear in the time averaged spectrum. Besides, the spectrum at $Ra = 7.0\times10^6$ has several peaks at higher wave numbers describe transient plumes as well as energy spectrum density at (a) $Ra = 8.8\times10^5$. But the variation of energy has clear difference between them. The former ones have clear threshold to separate larger and smaller structures, but the latter shows continuous envelope as also mentioned at the averaged spectra.

Velocity fluctuations observed in the velocity map (Fig.2) with low frequencies are consistent with the previous studies [3]. In thermal turbulence, they are caused by a thermal boundary layer instability triggered

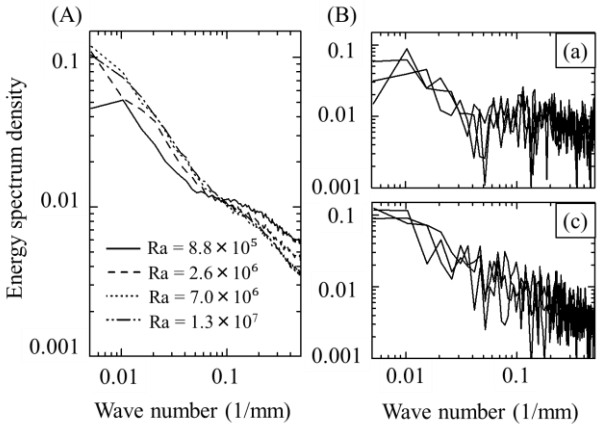

Figure 3(A): Average of energy spectral densities obtained at each time step, at each *Ra* . $Ra = 8.8\times10^5$ (solid line), 2.6×10^6 (dash line), 7.0×10^6 (dot line) and 1.3×10^7 (dash dot dash line). (B): Temporal energy spectrum densities at 264s, 500s and 764s at (a) and at 250s, 500s and 750s at (c).

by incoming transient plumes which are transported in

fluid layers [4]. In this study, velocity and temperature fluctuations with frequencies in the order of 10^{-3} Hz have some spectral peaks at each Rayleigh number as shown in Figure 4 (A). It indicates the fluctuation by a thermal boundary layer instability in the point of the order. In addition to these fluctuation, the spectrum at $Ra = 1.3\times10^7$ has a dominant peak at much lower frequency 0.0014Hz .

Figure 4 (B) shows the periods of these oscillations plotted, τ, normalized by thermal diffusion time, L^2/κ against Rayleigh number, where the open symbols represent periods corresponding to dominant peaks in power spectrum of velocity map, and solid symbols periods calculated from frequencies of temperature fluctuations. A solid line indicates the variation of periods extrapolated from the previous study with temperature measurements in the time dependent flow regime at which cellular convection emerges [3]. The obtained period agree with the extrapolation at $Ra = 8.8\times10^5$, and the periods obtained at larger Ra numbers have large gap against the extrapolation. This is because that large scale flows emerge and transport transient plumes all around the box for $Ra \geq 2.6\times10^6$: behaviors of the thermal plumes are dominated by large scale circulation, not by thermal boundary layer instability and the periods become longer. Variation of the periods tends to decrease as increasing Rayleigh number for $Ra \geq 2.6\times10^6$, because the magnitude of velocity of transient plumes become larger. Therefore, the fluctuation with a much longer period $\tau\kappa/L^2 = 0.069$ (0.0014 Hz in frequency) at $Ra = 1.3\times10^7$ seems isolated and is not a kind of ones by transient plumes. To characterize such long-term fluctuations observed at $Ra = 1.3\times10^7$, a long-term recording is performed as detailed in the next section.

3.3 Fluctuation of large scale flows

Figure 5 shows the time-space velocity maps of the flow for 4000 s measured by the Ch2 at $Ra = 1.3\times10^7$. As reported in the section 3.1, there are separated large scale flows and drift local structures organized by transient plumes for each direction. Advections of the local structures are represented by thinner stripes on the velocity map and these have a fluctuation with a period $\tau\kappa/L^2 = 0.01$ (0.01 Hz in frequency). In addition to this, there are thicker band on the map and it fluctuates with a period $\tau\kappa/L^2 = 0.09$ (0.001Hz). This motion of large scale flow is considered to be affected by the lateral wall of moderate aspect ratio box. Characterizing this meandering motion is ultimate goal of this study.

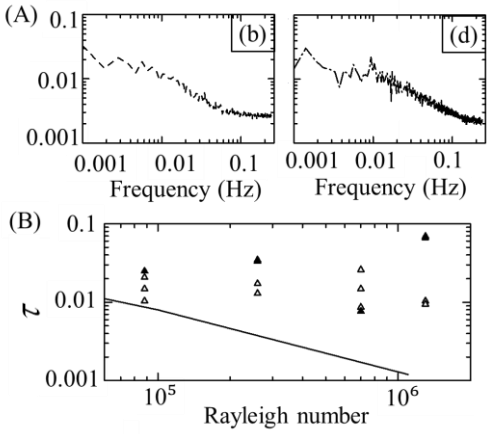

Figure 4: (A) Power spectrum density at (b) $Ra = 2.6\times10^6$ and (d) $Ra = 1.3\times10^7$ (B):The periods against Rayleigh number. (open symbols) periods corresponding to dominant peaks in power spectrum of velocity map. (solid symbols) periods calculated from frequencies of temperature fluctuations. (a solid line) the extrapolation from previous studies [3].

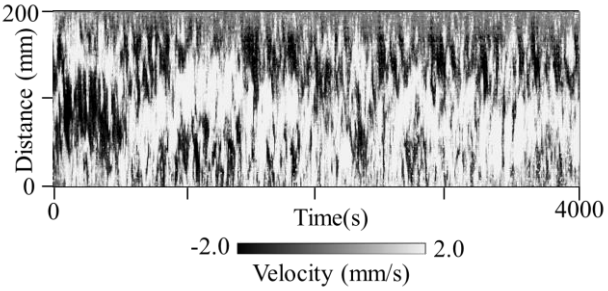

Figure 5: Time-space velocity map of the horizontal flow velocities obtained by Ch2 for 4000 s at $Ra = 1.3\times10^7$

4. Conclusion

The spatiotemporal velocity maps obtained by UVP at four Rayleigh numbers were investigated to elucidate transition of spatiotemporal structures of thermal turbulence confined by a moderate aspect ratio box. In the case of $Ra = 8.8\times10^5$, 3-D cellular structures are indistinctly organized by transient plumes. At $Ra = 2.6\times10^6$ and 7.0×10^6, local structures are carried in a direction and it indicates the emergence of large scale flow. As reached $Ra = 1.3\times10^7$, large scale flow is divided to several pieces and their arrangement changes in time. A comparison of spectra represents the transition as the change on spectral shape. The spatial spectra at the smallest Ra have clear gaps of energy between large and small scales of the flow. The others have almost simple decrease of the energy from large to small scales with several peaks representing local structures. In addition to the consistent oscillation, the much longer term fluctuation is dominant in power spectrum at $Ra = 1.3\times10^7$. It indicates the motion of large scale flows at the long-term recording and it is considered to be the effect of the lateral walls of a moderate aspect ratio box.

References

[1] Krishnamurti R & Howard LN: Large-scale flow generation in turbulent convection, Proc Natl. Acad. Sci. USA, 78 (1981)

[2] Sugiyama K, *et al*.: Flow Reversals in Thermally Driven Turbulence, Phys. Rev. Lett, 105(2010)

[3] Krishnamurti R: On the transition to turbulent convection. Part2. The transition to time-dependent flow, J. Fluid Mech., 42(1970)

[4] Qiu X-L *et al*.: Large-scale coherent rotation and oscillation in turbulent thermal convection, Phys. Rev. E, 61(2000)